Journal of
Photonics for Energy

PhotonicsforEnergy.SPIEDigitalLibrary.org

Directional control of narrow-band thermal emission from nanoantennas

Bowen Yu
Jiayu Li
Sheng Shen

SPIE.

Bowen Yu, Jiayu Li, Sheng Shen, "Directional control of narrow-band thermal emission from nanoantennas," *J. Photon. Energy* **9**(3), 032712 (2019), doi: 10.1117/1.JPE.9.032712.

Directional control of narrow-band thermal emission from nanoantennas

Bowen Yu, Jiayu Li, and Sheng Shen*
Carnegie Mellon University, Department of Mechanical Engineering, Pittsburgh, Pennsylvania, United States

Abstract. We investigate the directional control of narrow-band perfect thermal emission using a nanoscale Yagi–Uda antenna. Although Yagi–Uda antennas were demonstrated to achieve directional control in the optical and radio frequency regimes, they have not been applied for thermal infrared emission. Here, by coupling a nanoscale thermal emitter into a Yagi–Uda antenna, we demonstrate strong directional control of thermal emission with a narrow-band spectrum at the nanoscale. By exploring the effects of the reflector and the director of a Yagi–Uda antenna, the forward emission enhancement factor up to 8.3 is achieved through geometry optimization. © *2019 Society of Photo-Optical Instrumentation Engineers (SPIE)* [DOI: 10.1117/1.JPE.9.032712]

Keywords: thermal radiation; Yagi–Uda antenna; directional control.

Paper 18138SS received Dec. 3, 2018; accepted for publication Jan. 16, 2019; published online Feb. 5, 2019.

1 Introduction

The spectral and directional control of thermal emission remains challenging because thermal radiation is generally spatially and spectrally incoherent. However, by utilizing nanostructures, it has been recently demonstrated that thermal radiation can have both spatial and spectral coherence. Costantini et al.[1] used plasmonic metasurfaces to realize the directional and frequency-selective thermal emission. Ribaudo et al.[2] showed that two-dimensional silicon structures can emit highly directional thermal emission. Campione et al.[3] experimentally achieved directional and monochromatic thermal emission at epsilon-near-zero conditions in semiconductor hyperbolic metamaterials.

As highly directional emitting structures, Yagi–Uda antennas have been investigated and widely used for decades.[4–11] A Yagi–Uda antenna usually consists of a single driven element as the feed, a reflector, and several directors on either side of the feed to optimize and control the directionality of electromagnetic emission. With both continuous device miniaturization and growing demand on precise control of directionality, nanoscale Yagi–Uda antennas become increasingly important.[12–18] Kosako et al.[19] experimentally demonstrated the directional light emission from a nano-optical Yagi–Uda antenna composed of an array of finely tuned gold nanorods. Taminiau et al. numerically showed that the interaction of a single quantum emitter with electromagnetic fields can be enhanced by coupling with resonant plasmon modes in the near field. The angular emission of the coupled system is highly directed and determined by the design of the nanoscale Yagi–Uda antenna.[20] Although these nanoscale Yagi–Uda antennas have achieved the directional control in the traditional optical and radio frequency regimes, the directional control of thermal emission with a narrow-band spectrum remains a challenge.

In this work, we investigate the directional control of narrow-band perfect thermal emission using a nanoscale Yagi–Uda antenna consisting of an array of nanowires via numerical simulations. Based on nanoscale transmission line resonators as well as the design of Yagi–Uda antennas,[21] we numerically demonstrate the directional tunablity of the narrow-band thermal emission from a nanoscale Yagi–Uda antenna. Direct simulation of thermal emission is obtained by the Wiener chaos expansion method[22,23] and further optimized by our recently developed

*Address all correspondence to Sheng Shen, E-mail: sshen1@cmu.edu

1947-7988/2019/$25.00 © 2019 SPIE

quasi-normal mode (QNM) theory.[24] Our results clearly indicate that the nanoscale Yagi–Uda antenna array would be a promising component for the directional control of thermal infrared sources, infrared sensors, etc.

2 Optimization of Thermal Emission from a Single Nanoscale Emitter

While fluctuational electrodynamics lays a solid theoretical foundation for understanding any thermal radiation phenomena at thermal equilibrium,[25] the recently developed QNM theory provides a powerful tool to accurately describe the resonance modes in lossy and dispersive materials.[24,26] For a thermal emitter with a predominant resonance mode, we have employed QNM theory to show that thermal emission power $\phi(\omega)$ of the thermal emitter has the peak height $\phi(\omega) = \frac{\Theta}{2\pi} 4\eta_E \eta_\infty$ near its resonant frequency, where Θ is the Planck distribution, and η_E and η_∞ are the fractional mode losses in the emitter and to the far-field, respectively, which can be defined purely by the resonant mode profile solved from the QNM theory.[24] Here, η_E and η_∞ can be understood as the percentage of the mode energy dissipated inside the emitter and to the far-field, respectively, and $\eta_E + \eta_\infty = 1$. Hence, the upper limit of $\phi(\omega)$ equals $\frac{\Theta}{2\pi}$ when the mode losses are matched, i.e., $\eta_E = \eta_\infty = 0.5$.

The shape of the thermal emission spectrum is approximated by the Lorentz function. $L(\omega) = \frac{Re^2(\omega_n)}{Re^2(\omega_n) + 4Q_n^2[Re(\omega_n) - \omega]^2}$,[24] where ω_n is the complex resonant frequency of the QNM and $Q_n = |\frac{Re(\omega_n)}{2Im(\omega_n)}|$ is the quality factor of the QNM. Here, we choose a gold nanorod thermal emitter as the feed in our Yagi–Uda antenna design. For this kind of metallic subwavelength resonators, its QNM profile follows the configuration of Fabry–Pérot resonance modes.[21] Consequently, its resistive loss is closely related to the material properties and cross-section sizes, and its radiative loss is determined by the length of the emitter. In fact, the fundamental mode of its QNMs behaves like dipole-radiation as shown in Fig. 1(a) for the spatial distribution and Fig. 1(b) for the spectral thermal emission. We use the reduced heat flux ϕ to represent the thermal radiation, where the actual thermal radiation power that propagates into the far field is given by $\Phi = \int \frac{d\omega}{2\pi} \frac{\phi(\omega)}{A} \Theta(T_a, \omega)$, where A is the surface area of the emitter and T_a is the temperature of the emitter. Here, we apply the fluctuating surface current method[27–29] to optimize the gold nanorod emitter at the wavelength of 7.25 μm. The corresponding optimized geometry parameters are 40 nm for width, 40 nm for thickness, and 2.5 μm for length. In the

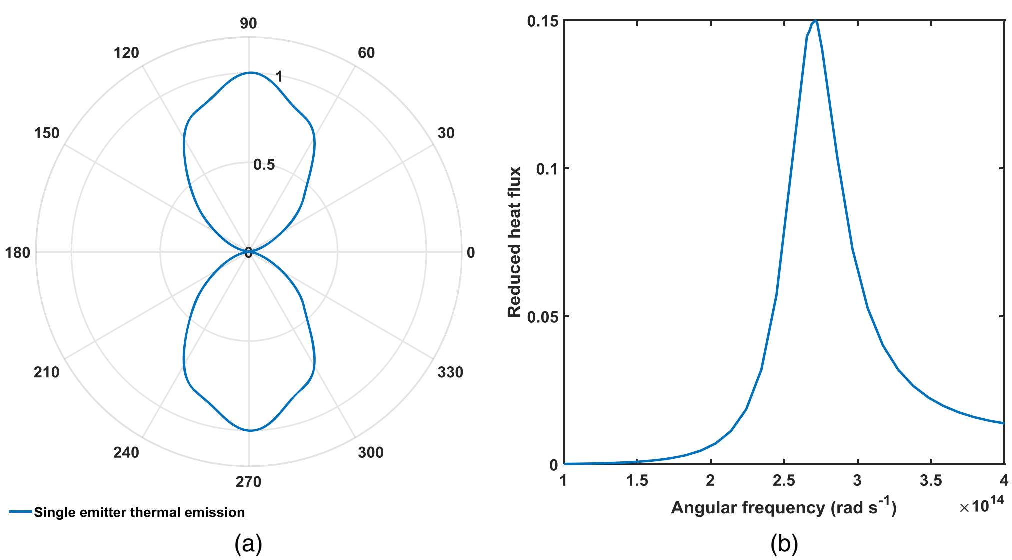

Fig. 1 (a) Spatial distribution of the far-field thermal emission from a single gold nanorod emitter. The plotted physical quantity is the normalized $|E|^2$ with respect to the peak intensity. (b) Spectral thermal emission from the single gold nanorod emitter where the resonant wavelength is located around 7.25 μm.

following sections, we will use this designed gold nanorod emitter as the feed of the Yagi–Uda antenna.

3 Directional Thermal Emission from Nanoscale Yagi–Uda Antennas

In general, a Yagi–Uda antenna array consists of a reflector, a feed, and multiple directors, as shown in Fig. 2. The directionality of the Yagi–Uda antenna array mainly originates from the constructive interference of the propagating electromagnetic waves. The suppression of the backward propagation by the reflector also contributes to the directionality. Although thermal radiation is generally considered to be incoherent due to its stochastic feature, the introduction of the optimized QNM within a single thermal emitter could compensate the lack of coherence and facilitate the design of the whole Yagi–Uda antenna array. The surface plasmonic modes along the gold nanorod emitter increase the spatial coherence of its thermal emission. By optimizing the QNMs to make it spectrally narrow and sharp, the temporal coherence can be improved as well. Therefore, the concept of constructive interference of electromagnetic waves can still work properly in the thermal Yagi–Uda antenna. Yet, due to the randomness inherited in thermal radiation, the directionality of the thermal Yagi–Uda antenna expect to be weaker than that of the radio frequency or optical Yagi–Uda antenna. The challenge for designing a high-performance thermal Yagi-Uda antenna is twofold. One is that the forward emission enhancement is less strong compared to optical antennas given its low coherence. The other is that the resulting contrast between the forward and the backward emission is small due to the weak suppression on the backward emission.

To quantitatively evaluate the performance of the directional control of a thermal Yagi–Uda antenna, we directly calculate the half-height emission angle φ and the forward and the backward emission enhancement factors I_F and I_B in terms of the thermal radiation field intensity $|E_0|^2$ of the single emitter, namely $I_{F,B} = |E_{F,B}|^2/\ |E_0|^2$.

Here, we address the impact of the directors and the reflectors on the thermal emission pattern of the Yagi–Uda antenna. By sweeping the geometry parameters of the antenna including director length, spacing distance, reflector length, and height, we obtain the optimized Yagi–Uda antenna design at the interested wavelength.

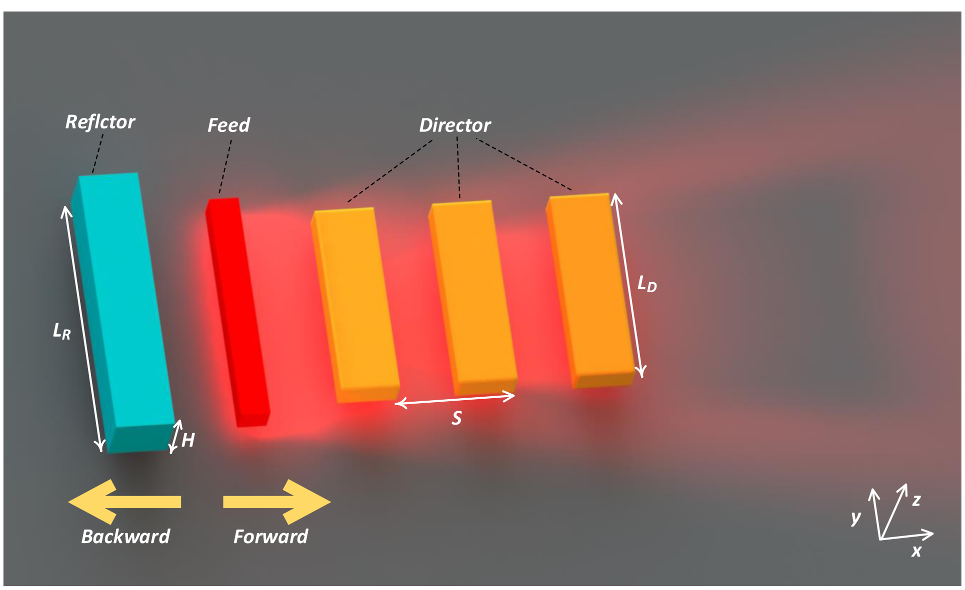

Fig. 2 Schematic of a Yagi–Uda antenna with one feed, one reflector and three directors. L_R, H, L_D, and S denote the length of the reflector, the height of the reflector, the length of the directors, and the spacing between the directors, respectively.

3.1 *Spacing of the Directors*

The distance between the neighboring directors is the most crucial parameter in controlling the directionality of the Yagi–Uda antenna. As the enhancement of the forward emission lies in the constructive interference of propagating waves, the spacing between the neighboring directors can significantly modify the forward emission by altering the relative phase of the adjacent directors. In the scenario of thermal radiation, the reflector and all the directors will simultaneously become secondary thermal sources once the feed emitter is thermally activated. As long as the spacing falls in the resonant wavelength of the feed which is 7.25 μm in our case, the secondary thermal emission could interfere with each other either constructively or destructively. We choose the length of each director to be 2.2 μm and with the cross-section area of 40 nm by 100 nm. The reflector is 3 μm long and separated from the feed by 1.8 μm. The total number of the directors next to the feed is assumed to be 3. Figure 3(a) plots the thermal emission pattern of the Yagi–Uda antenna for the spacing S in the range of 500 nm to 6 μm, whereas Fig. 3(b) represents the forward and the backward emission intensity enhancement factors. The forward emission intensity gradually increases with the increasing spacing and reach the maximum when S is equal to 3 μm, thus imposing strong constructive interference. The backward emission intensity shows a similar trend but experiences the suppression from the reflector due to the quarter-wavelength phase shift between the feed and itself. It is worth noting that the half-height emission angle φ does not vary much with the spacing. For all our calculations, the half-height emission angle maintains around 62 deg for the forward emission and 55 deg for the backward emission.

3.2 *Length of the Directors*

The length of the directors is another important factor for the directionality of the Yagi–Uda antenna. As described in the previous section, the directors could become secondary thermal sources and contribute to the final emission pattern. The length of the directors turns out to be the dominant parameter in determining the resonant wavelength. It seems that the ideal case in terms of the forward emission intensity should be that the length of the directors is equal to the feed's length. However, in choosing the same length for both the directors and the feed, the backward emission will also be boosted. So, it is necessary to avoid such resonance between the feed and the directors. Here, we calculate the thermal emission of the Yagi–Uda

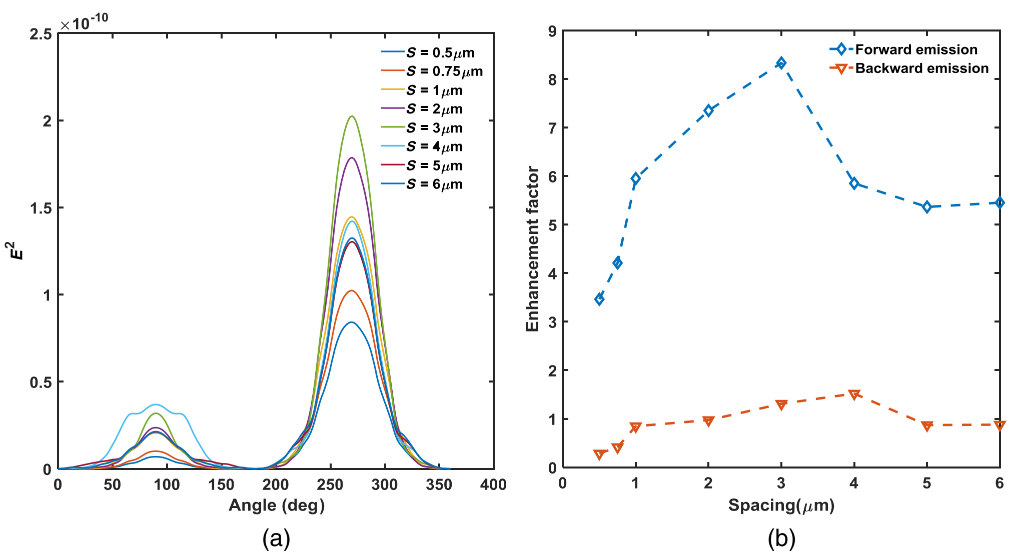

Fig. 3 (a) Spatial distribution of the thermal emission projected to the XY plane at different director spacings. (b) Enhancement factors of the forward (270 deg) and the backward (90 deg) emission. The calculation of the enhancement factors is based on the thermal radiation signal from the feed only.

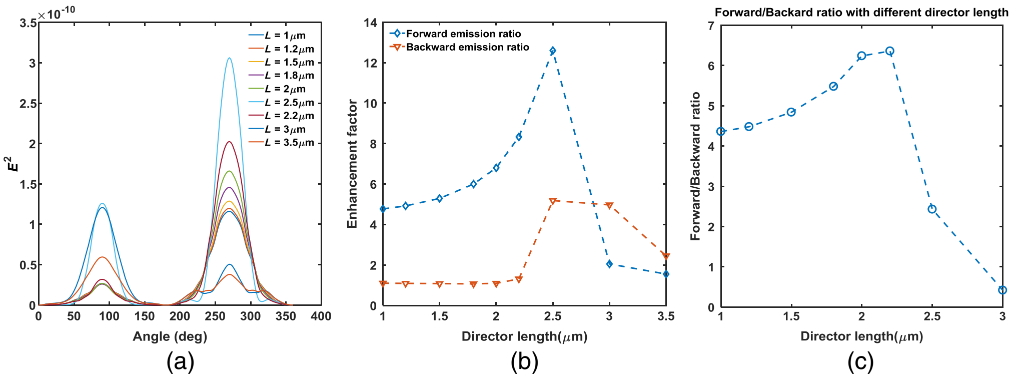

Fig. 4 (a) Spatial distribution of the thermal emission projected to the XY plane with different director lengths. (b) Enhancement factors of the forward (270 deg) and the backward (90 deg) emission. The calculation of the enhancement factors is based on the thermal radiation signal from the feed only. (c) Forward/backward ratio under different director lengths.

antenna with different lengths of the directors. The parameter of the reflector is the same as that described in Sec. 3.1. The total number of the directors is still 3 and the spacing is now fixed to be 3 μm. The corresponding thermal emission pattern and emission intensity enhancement factors are plotted in Fig. 4. From Fig. 4(b), we can see that the forward emission indeed reaches the strongest point at the length of 2.5 μm. But the backward emission intensity also becomes the highest. The forward/backward ratio is plotted in Fig. 4(c). The ratio of the forward and the backward emission intensities at the length of 2.5 μm in this case is obviously worse than other cases. It should also be pointed out that the backward emission becomes dominant when the length of the directors is larger than 2.5 μm, as shown in Fig. 4(a). As a result, the optimal length of the director should be slightly smaller than the feed's length, which is 2.2 μm in this case.

3.3 *Influence of the Reflector*

The role of the reflector in the Yagi–Uda antenna is to suppress the backward emission. To realize it, the reflector should be placed at a distance of approximately one-fourth resonant

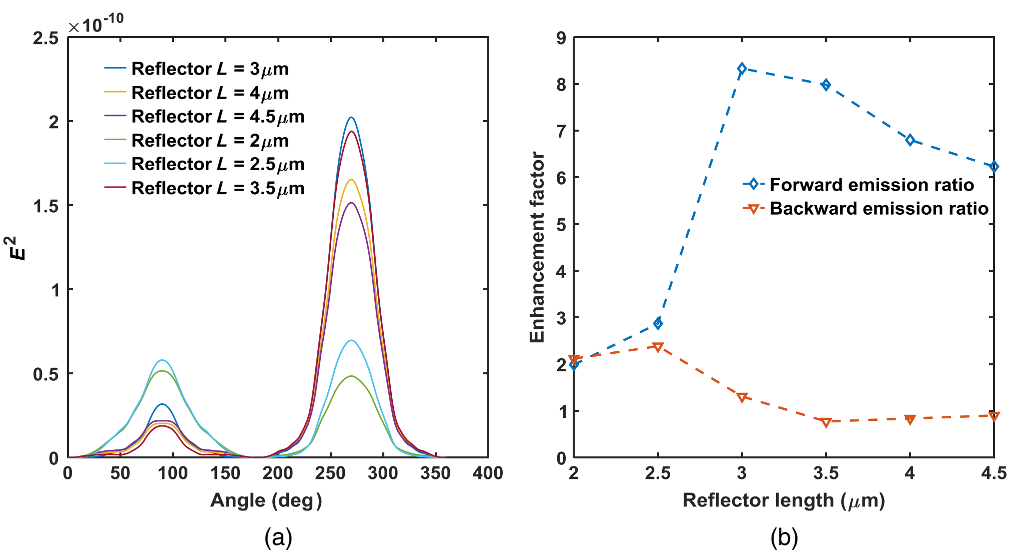

Fig. 5 (a) Spatial distribution of the thermal emission projected to the XY plane with different reflector lengths. (b) Enhancement factors of the forward (270 deg) and the backward (90 deg) emission. The calculation of the enhancement factors is based on the thermal radiation signal from the feed only.

wavelength from the feed. The π phase shift generated by the quarter-wavelength gap could therefore effectively destruct the backward emission. On the other hand, the length of the reflector should be larger than that of the feed in order to block the direct thermal radiation coming from the feed. The length of the reflector turns out to be an important parameter in optimizing the antenna directionality. Here, we calculate the thermal emission pattern and emission intensity with different reflector lengths. As shown in Fig. 5(b), the antenna gives the best performance when the reflector length is 3 μm which is slightly larger than that of the feed. As the reflector length becomes larger, it further suppresses the backward emission below the emission of the single emitter. When the reflector length is smaller than the feed length, the antenna begins to

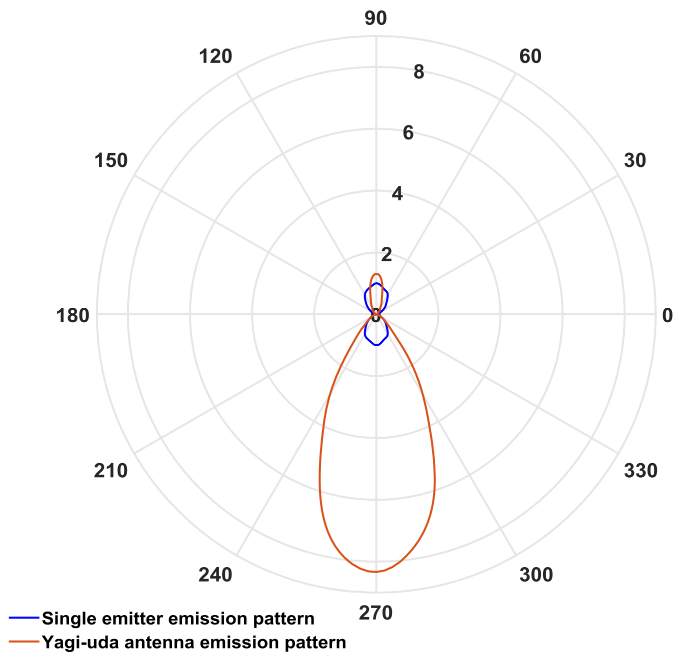

Fig. 6 Spatial distribution of thermal emission from a single-gold nanorod emitter and the Yagi–Uda antenna.

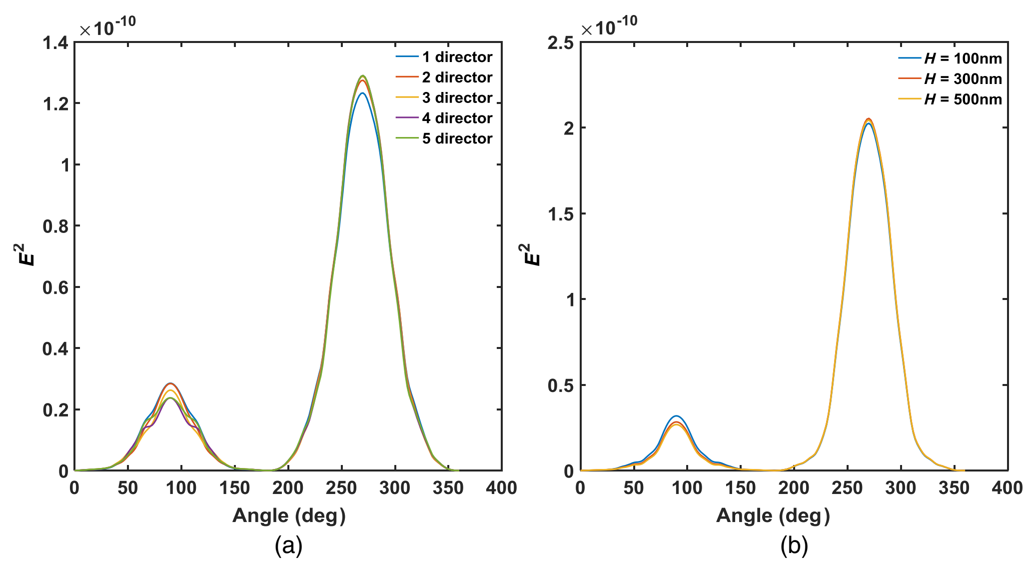

Fig. 7 (a) Spatial distribution of the thermal emission projected to the XY plane with different numbers of directors. (b) Spatial distribution of the thermal emission projected to the XY plane with different reflector heights.

enhance both the forward and the backward emission and lose the directionality. The decrease of the forward emission when increasing the reflector length is due to the shift of the resonant wavelength from the reflector. Therefore, the reflector length should be chosen to be slightly larger than the feed length. Finally, we can plot the spatial distribution of the thermal emission from the optimized Yagi–Uda antenna in comparison with the single nanorod emitter in Fig. 6, where an enhancement factor of the forward emission up to 8.3 is achieved.

There exist some other parameters affecting the design of the Yagi–Uda antenna, such as the total number of the directors and the height of the reflector. In Fig. 7, we show that these two parameters play a minor role in the performance of the antenna. For the number of the directors, even one director is enough to enable the directionality because the director nearest to the feed is the one most strongly activated, as shown in Fig. 7(a). For the height of the reflector, given that the spatial distribution of thermal emission is more oriented in the longitudinal direction, its influence on the directionality is negligible.

4 Conclusion

In conclusion, the optimal design of the thermal Yagi–Uda antenna varies with the wavelength of interest. For a given resonant wavelength, the spacing between the directors should be around half of the wavelength. The director length should be slightly smaller than the feed length, whereas the reflector length should be slightly larger than the feed length. For the optimized Yagi–Uda antenna in this work, an enhancement factor of the forward emission up to 8.3 is achieved. Hence, nanoscale Yagi–Uda antenna arrays would be a promising platform for controlling the directionality of thermal infrared sources.

Acknowledgments

This work was supported by the Defense Threat Reduction Agency (Grant no. HDTRA1-18-1-0046).

References

1. D. Costantini et al., "Plasmonic metasurface for directional and frequency-selective thermal emission," *Phys. Rev. Appl.* **4**(1), 014023 (2015).
2. T. Ribaudo et al., "Highly directional thermal emission from two-dimensional silicon structures," *Opt. Express* **21**(6), 6837–6844 (2013).
3. S. Campione et al., "Directional and monochromatic thermal emitter from epsilon-near-zero conditions in semiconductor hyperbolic metamaterials," *Sci. Rep.* **6**, 34746 (2016).
4. C. A. Balanis, "Antenna theory: a review," *Proc. IEEE* **80**(1), 7–23 (1992).
5. L. Z. Zheng and D. N. C. Tse, "Diversity and multiplexing: a fundamental tradeoff in multiple-antenna channels," *IEEE Trans. Inf. Theory* **49**(5), 1073–1096 (2003).
6. L. C. Godara, "Application of antenna arrays to mobile communications. II. Beam-forming and direction-of-arrival considerations," *Proc. IEEE* **85**(8), 1195–1245 (1997).
7. D. S. Shiu et al., "Fading correlation and its effect on the capacity of multielement antenna systems," *IEEE Trans. Commun.* **48**(3), 502–513 (2000).
8. Y. W. Hsu et al., "Dual-polarized quasi Yagi–Uda antennas with End Fire radiation for millimeter-wave MIMO terminals," *IEEE Trans. Antennas Propag.* **65**(12), 6282–6289 (2017).
9. H. Galal and M. Agio, "Highly efficient light extraction and directional emission from large refractive-index materials with a planar Yagi–Uda antenna," *IEEE Opt. Mater. Express* **7**(5), 1634–1646 (2017).
10. F. Liang et al., "Beam-scanning microstrip quasi-Yagi–Uda antenna based on hybrid metal-graphene materials," *IEEE Photonics Technol. Lett.* **30**(12), 1127–1130 (2018)
11. S. Wang et al., "Analysis and design of sea-water monopole Yagi–Uda antenna with pattern reconfigurability," *Int. J. RF Microwave Comput. Aided Eng.* **28**, e21399 (2018).
12. K. B. Crozier et al., "Optical antennas: resonators for local field enhancement," *J. Appl. Phys.* **94**, 4632–4642 (2003).

13. P. J. Schuck et al., "Improving the mismatch between light and nanoscale objects with gold bowtie nanoantennas," *Phys. Rev. Lett.* **94**, 017402 (2005).
14. P. Mühlschlegel et al., "Resonant optical antennas," *Science* **308**, 1607–1609 (2005).
15. D. P. Fromm et al., "Gap-dependent optical coupling of single 'bowtie' nanoantennas resonant in the visible," *Nano Lett.* **4**, 957–961 (2004).
16. S. Arslanagic and R. W. Ziolkowaski, "Highly subwavelength, superdirective cylindrical nanoantenna," *Phys. Rev. Lett.* **120**, 237401 (2018).
17. W. Rieger et al., "Yagi–Uda nanoantenna enhanced metal-semiconductor-metal photodetector," *Appl. Phys. Lett.* **113**, 023102 (2018).
18. A. Vaskin et al., "Directional and spectral shaping of light emission with Mie-resonant silicon nanoantenna arrays," *ACS Photonics* **5**, 1359–1364 (2018).
19. T. Kosako, H. F. Hofmann, and Y. Kadoya, "Directional control of light by a nano-optical Yagi–Uda antenna," *Nat. Photonics* **4**, 312–315 (2010).
20. J. N. Farahani et al., "Single quantum dot coupled to a scanning optical antenna: a tunable superemitter," *Phys. Rev. Lett.* **95**, 017402 (2005).
21. B. A. Liu et al., "Perfect thermal emission by nanoscale transmission line resonators," *Nano Lett.* **17**, 666–672 (2017).
22. J. Y. Li, B. A. Liu, and S. Shen, "Tunable narrow-band near-field thermal emitters based on resonant metamaterials," *Phys. Rev. B* **96**, 075413 (2017).
23. B. A. Liu and S. Shen, "Broadband near-field radiative thermal emitter/absorber based on hyperbolic metamaterials: direct numerical simulation by the Wiener chaos expansion method," *Phys. Rev. B* **87**, 115403 (2013).
24. B. A. Liu, J. Y. Li, and S. Shen, "Resonant thermal infrared emitters in near-and far-fields," *ACS Photonics* **4**(6), 1552–1557 (2017).
25. S. M. Rytov, Y. A. Kravtsov, and V. I. Tatarskii, Principles of statistical radiophysics, Vol. **3**, Springer-Verlag, Berlin (1989)
26. C. Sauvan et al., "Theory of the spontaneous optical emission of nanosize photonic and plasmon resonators," *Phys. Rev. Lett.* **110**, 237401 (2013).
27. B. A. Liu, Y. M. Liu, and S. Shen, "Thermal plasmonic interconnects in graphene," *Phys. Rev. B* **90**, 195411 (2014).
28. A. W. Rodriguez, M. T. H. Reid, and S. G. Johnson, "Fluctuating-surface-current formulation of radiative heat transfer: theory and applications," *Phys. Rev. B* **88**, 054305 (2013).
29. J. Y. Li, B. A. Liu, and S. Shen, "Graphene surface plasmons mediated thermal radiation," *J. Opt.* **20**(2), 024011 (2018).

Biographies of the authors are not available.